Process Technology for the Continuous Hot Band Annealing of 17%Cr Ferritic Stainless Steel

B.K. Jha, P. Jha, and C.D. Singh

(Submitted 2 February 2001)

As an alternative to time- and energy-consuming batch annealing, process technology for the continuous hot band annealing of 17%Cr ferritic stainless steel has been established. Process parameters (i.e., temperature and time) for the hot band annealing were optimized in the laboratory and, subsequently, plant trials were conducted. The impact toughness value of the annealed hot band was found to be the most crucial parameter to assess the cold rollability in the commercial run. When the hot bands were continuously annealed at 900 °C, the improved impact toughness values resulted in successful cold rolling to the desired thickness. The impact toughness value and subsequent cold rollability were found to be related to the formation of martensite volume%. Annealing the hot band in the lower temperature range of the two-phase ($\alpha + r$) region (i.e., 900 °C) yielded the best result. Improvement in roping index has been reported as a result of the weakening of the texture of the continuous-annealed hot band.

Keywords batch annealing, continuous annealing, ferritic stainless steel, hot band, impact toughness, microstructure, texture

1. Introduction

Against the background of social needs for saving natural resources and energy, 17%Cr ferritic stainless steels have experienced a large growth in demand for domestic and industrial appliances. These demands have resulted from the fact that the ferritic stainless steels have a relatively low cost, good corrosion resistance, and esthetically pleasing appearance. The normal process for the manufacture of these steel strips, adopted worldwide today, consists of continuously casting into slabs, hot rolling the slabs into strips, batch annealing the hot bands in the box furnaces (BAF) at the temperature range of 820-850 °C for a total period of 50 h, pickling the annealed hot bands, cold rolling to final gauges in single or double stages, and, finally, continuously annealing and pickling before they are skin passed as finished products. Of all the processes involved in the commercial production of these steel strips, the BAF process is the most time- and energy-consuming, and in order to meet the fast-growing market demand, the development of a highly productive annealing process[1,2] in a continuous annealing furnace (CAF) has been needed. Thus far, such a process has been successfully commercialized in the case of Ti-added ferritic stainless steels[3,4] only.

Furthermore, the cold-rolled and annealed strips processed through the BAF route suffer from low drawability and high roping, and both require optimization of texture components at each level of processing for their improvement, particularly at the stage of hot band annealing. It is clear that the drawability (Lankford parameter) and the roping phenomenon are the result of anisotropic flow of mixed textures, and that the origin of these textures may be traced to textural and microstructural banding during hot rolling.[5-7] Thus, the elimination of the textural and the microstructural banding in the annealed hot band is an essential step for improving the drawability and the roping phenomenon.[8-18] This requires, in turn, the optimization of hot band annealing to make the material suitable for cold rolling. This software technology is still untapped and has some industrial importance toward the development of continuous annealing of the hot band (HB) in a continuous annealing furnace.

Our intention is the development of the continuous annealing technology for 17%Cr stainless steel strip as well as the optimization of the hot band annealing texture components. These are the bases of the experiments and trials presented in this paper.

2. Experimental

The commercially produced hot-rolled bands of steel grade AISI 430 with nominal composition (wt.%) 0.05C, 0.45Mn, 0.20Si, 0.02P, 0.001S, 16.8Cr, 0.03N, and 0.015% Al were used for the current investigation. Both laboratory (lab) experiments and plant trials were performed on these grades. For laboratory experiments, the HB strips (4.0 mm thick) were annealed in the single-phase (α) region at a temperature of 850 °C for 5 h and then furnace cooled to simulate the BAF process. Additionally, the CAF process was simulated by annealing the HB strips in both single-phase and two-phase ($\alpha + r$) regions (Fig. 1) at temperatures ranging from 860 to 1000 °C for a period of 3.0 min followed by quenching into water. The annealing time of 3.0 min was selected to simulate the continuous annealing condition where the residence heating time of the strip at a speed of 10 m/s is 3.0 min. The plant trials were conducted by annealing the HB strips in the continuous annealing furnace at a furnace temperature of 990 °C and 900 °C and at a speed of 6-10 meters per minute. The continuously annealed hot bands, after pick-

B.K. Jha, P. Jha, and **C.D. Singh,** Research and Development Centre for Iron and Steel, Steel Authority of India Ltd., Ranchi 834002, India. Contact e-mail: ske@rdcis.bih.nic.in.

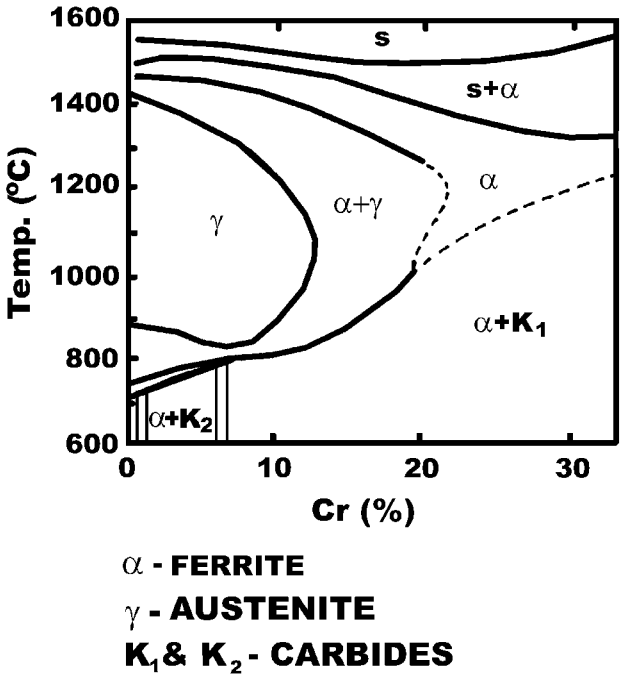

Fig. 1 Phase diagram of Fe-0.05C-Cr alloy

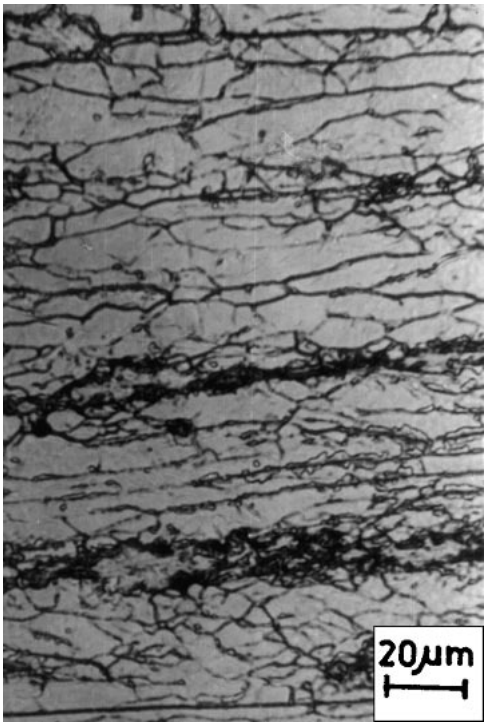

Fig. 2 Optical micrograph of longitudinal section at the central layer of the hot band

ling, were cold-rolled to final gauges in two stages. The first stage of processing, which consisted of 50% reduction in the Z-mill and of intermediate annealing at 850 °C at line speed of 8 meters per minute, was followed by the second stage of production comprising 75% reduction in the Z-mill, final annealing at 850 °C, and a line speed of 28 meters per minute.

The mechanical properties (Y.S., U.T.S., and percentage total elongation) of both laboratory-annealed hot bands and plant-processed materials (annealed hot bands and final cold-rolled and annealed strips) were determined by performing tensile tests at a strain rate of 6.7×10^{-4} per second. The plastic anisotropy (i.e., r and Δr) of the final product was obtained by straining the tensile specimen by 15% and determining the width to thickness true strain ratio for the specimens in 0 degree, 45 degree, and 90 degree orientation with respect to rolling direction. The roping index for the specimen parallel to rolling direction was also determined at the same strain level.[5] In all cases, the hardness (Rockwell B) values were obtained. Furthermore, the impact toughness of the annealed hot bands was evaluated by conducting charpy V-notch tests on nonstandard specimens ($55 \times 10 \times 4$ mm size).

The microstructural evaluation and the fractography analysis on selected specimens were conducted with the help of optical microscope and scanning electron microscope (SEM), respectively. On the other hand, the analysis of the texture components of the hot band and the annealed hot bands was carried out by determining {110}, {002}, {112}, and {103} incomplete pole figures using x-ray back-reflection technique[19] and also an orientation distribution function (ODF) technique[20,21], based on the series extended to $\ell = 22$ (i.e., even terms only). The ODF f (g) of the crystallites was determined in the Euler space ($0° \leq \Phi_1, \Phi, \Phi_2 \leq 90°$) and presented along the skeleton line (i.e., fiber) of texture orientation tubes.

3. Results and Discussion

3.1 Microstructure Evolution

Figures 2-5 show the microstructures of the longitudinal section at the central layers of hot band and the hot bands annealed at 850 °C, 900 °C, and 990 °C, respectively. While the first temperature simulates the BAF process, the latter two temperatures indicate the simulation of the CAF process. The most interesting feature of the hot band microstructure is the presence of bands of ferrite and martensite, particularly, the latter phase at the interband and interferritic boundaries along the rolling direction. Further, there are indications of an advanced stage of recrystallization within the ferrite bands and at band boundaries. The average volume fraction of martensite was about 18% and the measured hardness values of ferrite and martensite phases were about 179 HV and 470 HV, respectively.

The microstructure (Fig. 3) obtained as a result of single-phase annealing at 850 °C, indicates the decomposition of martensite into an aggregate of ferrite and carbides, presumably $M_{23}C_6$. Significantly, the prior γ-α and α-α′ boundaries are the preferred nucleation sites of carbides. Furthermore, there is precipitation of carbides within ferrite grains. Though some ferrite grains have grown, banding still exists. The persistence of banding is due to the restrictive growth as the ferrite boundaries are pinned up by the precipitation of carbides. On the other hand, the microstructure (Fig. 4) evolved as a result of two-phase annealing at 900 °C depicts that the martensite has just decomposed into aggregates of ferrite and carbides. The precipitation of carbides mostly on prior γ-α and α-α′

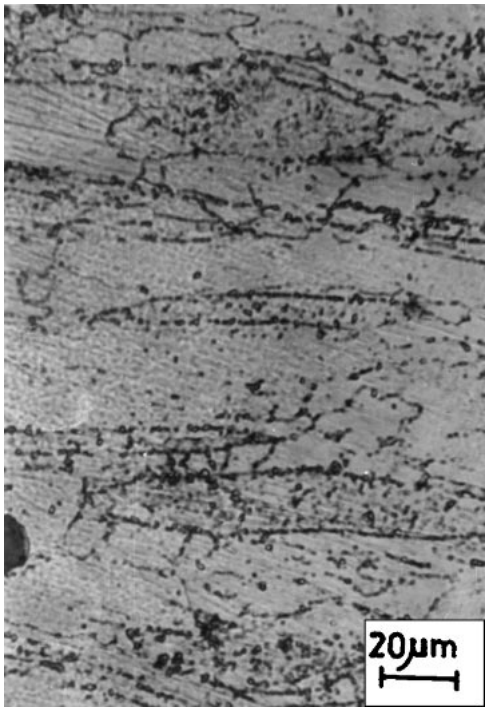

Fig. 3 Optical micrograph of longitudinal section at the central layer of single-phase annealed hot band (temperature 850 °C)

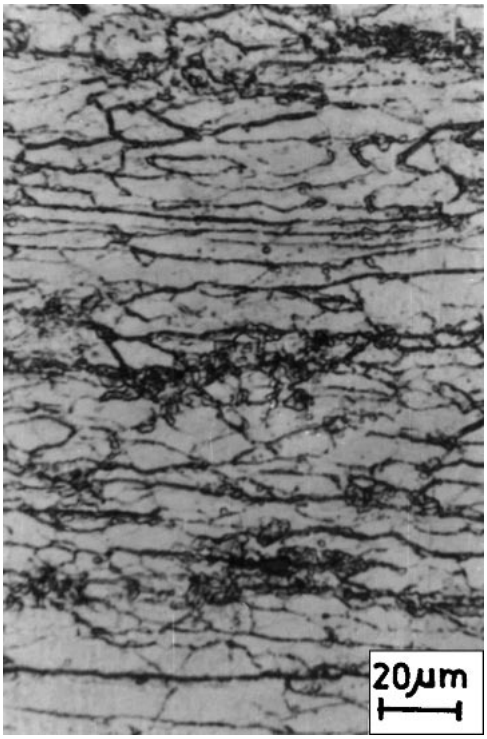

Fig. 4 Optical micrograph of longitudinal section at the central layer of two-phase annealed hot band (temperature 900 °C)

boundaries has resulted in the formation of carbide layers parallel to the sheet surface and thus prevented substantial grain growth. Though some austenite forms during annealing at 900 °C, all such austenite transforms to ferrite before quenching into water. In contrast, the two-phase annealing at the higher temperature of 990 °C has led to the formation of a substantial amount of austenite (volume fraction 25%) which, on quenching into water, transforms into martensite (Fig. 5). Furthermore, this annealing resulted not only in the formation of large ferrite grains, but also the retention of some more carbon into solid solution (i.e., supersaturation).

3.2 Texture Evolution

The ODF results indicate that the textures can be best described by three limited orientation tubes in the Eulerian space. The first orientation tube has its fiber axis <110> parallel to RD (<110>//RD) and runs from {001}<110> through {112}<110> to near {111}<110> with a maxima at ~{001}<110>, while the second orientation tube extends between {112}<110> and {111}<112> with its fiber axis <110> inclined about 30 degrees from ND toward RD (<110>30°ND) and its maxima at {112}<110>. The orientation {112}<110> is at the intersection point of these two limited fibers, that is, <110>//RD and <110>30°ND. The third orientation tube stretches from {001} <110> to {001} <100> and has its fiber axis <001> parallel to ND (<001>//ND) and maxima {001}<110>. The texture components {001}<110> lies at the joining point of the limited fibers <110>//RD and <001>//ND. Figures 6-8 depict the orientation density plots along <110>//RD, <110>30°ND, and <001>//ND fiber, respectively. The plots have been obtained for hot band and the hot bands annealed at 850 °C, 900 °C, and 930 °C.

It is clearly evident from these figures that the HB exhibits a strong hot-rolled texture described by <110>//RD, <110>30°ND, and <001>//ND fibers with an orientation peak density of decreasing order from ~{001}<110>, ~{112}<110>, ~{111}<110>, and ~{111}<112>. The latter two components are minor ones. The texture of the specimen shows, after single-phase annealing at 850 °C, essentially the same features as those observed in HB, although some texture components such as {112}<110> and {111}<112> are sharpened at the expense of the components of <001>//ND fiber and, in particular, of {001}<110> orientation. However, during annealing in single phase at 850 °C treatment, the orientation density of <110>30°ND fiber has increased considerably. On the other hand, the two-phase annealing at 900 °C has decreased the orientation density of all three orientation fibers to a large extent and also led to the development of new texture components {015}<100> and {023}<100>. In general, this two-phase annealing treatment has resulted in the randomization of the HB texture components. This randomization at the hot band annealing stage is desirable for improving the drawability and roping characteristics of the finished steel strips.[5-7] Interestingly, the two-phase annealing at still higher temperature (i.e., 930 °C) has led to the development of texture similar to that observed in the HB, that is, a phenomenon of texture memory.

3.3 Mechanical Properties and Fractography Evaluation

Figure 9 shows the changes in mechanical properties (i.e., Y.S., U.T.S., %EL, and hardness) of the HB as received and after annealing at different temperatures ranging from 860 °C

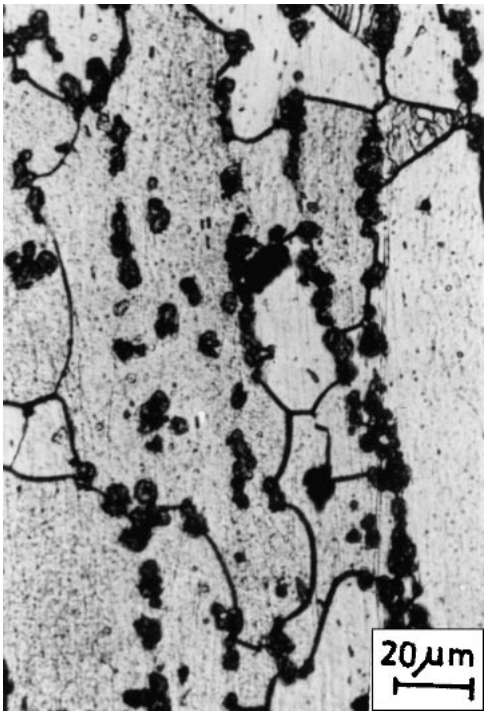

Fig. 5 Optical micrograph of longitudinal section at the central layer of two-phase annealed hot band (temperature 990 °C)

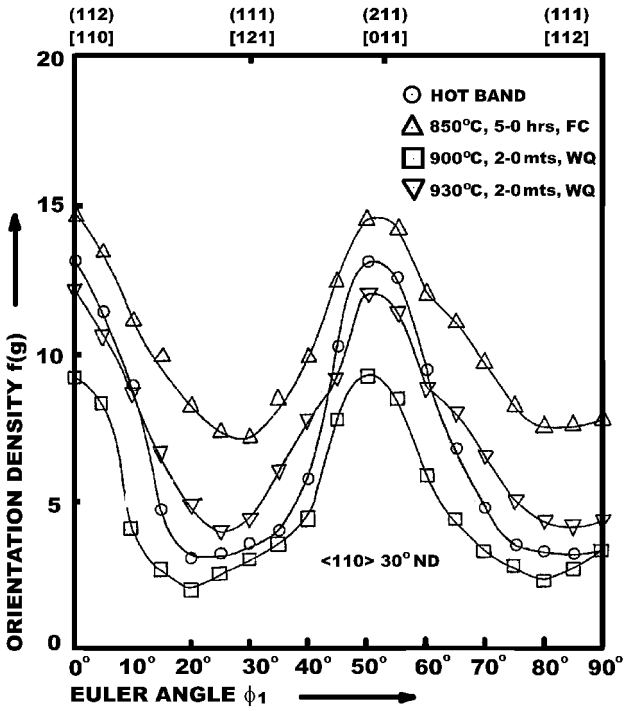

Fig. 7 Orientation density plot along <110>30°ND fiber

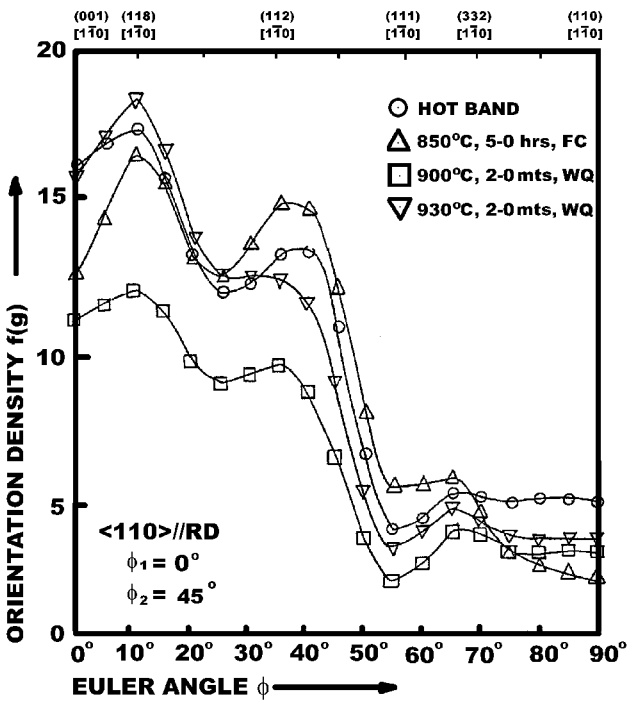

Fig. 6 Orientation density plot along <110>//RD fiber

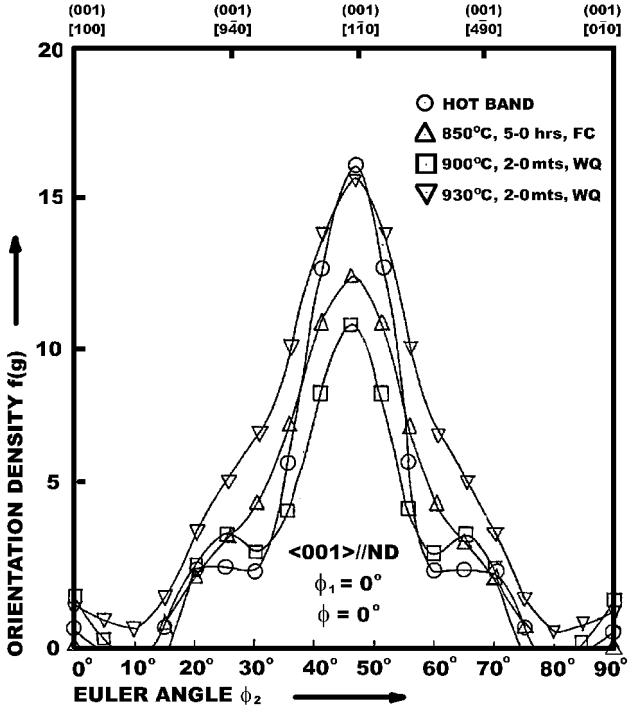

Fig. 8 Orientation density plot along <001>//ND fiber

to 1000 °C. One can easily recognize from Fig. 9 that no significant changes in mechanical properties occur between annealing temperatures of 860 to 940 °C. Above 940 °C, the Y.S., %El, and hardness values remain almost constant, whereas the U.T.S. value increases. This increase in U.T.S. value is the manifestation of increased rate of work hardening due to increase in the amount of second phase (i.e., martensite), while the consistent behavior of other mechanical properties

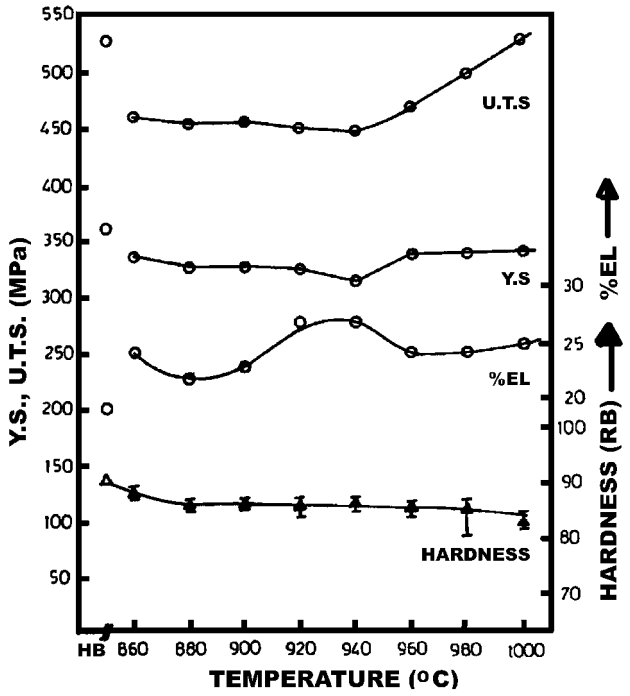

Fig. 9 Effect of annealing temperature on mechanical properties of hot band

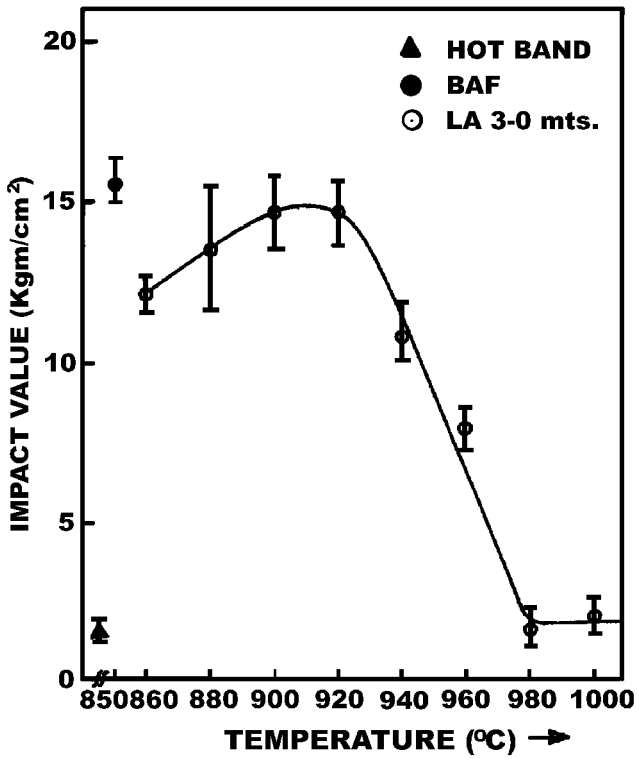

Fig. 10 Effect of annealing temperature on impact toughness value of hot band

reflects a balance between two processes (i.e., martensite formation and grain coarsening) that are opposite in nature. The evaluation of mechanical properties for the different annealing temperatures did not give any clue for selecting the annealing parameter for the continuous annealing in the plant. It was thus thought to carry out experiments to determine the impact value of HB after annealing at different temperatures.

Figure 10 depicts the impact value of various lab-annealed hot band samples. From annealing temperatures of 860 °C to 900 °C, there is an increasing tendency in the impact values (12.5 to 14.5 kg · m/cm^2) which remains almost constant to 920 °C. However, from an increasing annealing temperature above 920 °C, there is a sharp decrease of impact value until 980 °C. For comparison, the impact values of HB and BAF samples are also shown in the figure. It can be seen from the figure that the annealed samples from above 980 °C have impact values closer to that of HB (1.5 kg · m/cm^2). The maximum impact value of 14.5 kg · m/cm^2 was obtained for an annealing temperature of 900 °C and is closer to the impact value of 15.5 kg · m/cm^2 for the batch-annealed hot band. Impact value thus appeared to set a guideline for further rollability of annealed hot band, and thus two annealing temperatures of 900 °C and 990 °C were chosen for annealing the hot band in the continuous annealing line.

Figures 11-14 are the fractography of the laboratory-annealed samples. The fractographs have been taken from the region near the V-notch of the broken impact samples. Figures 11 and 12 (i.e, the fractographs of samples annealed at 860 °C and 900 °C, respectively) show that the fracture mode is predominantly ductile as represented by the presence of many dimples. At the annealing temperature of 940 °C, mixed mode of fracture is visible, as shown in Fig. 13. However, total brittle

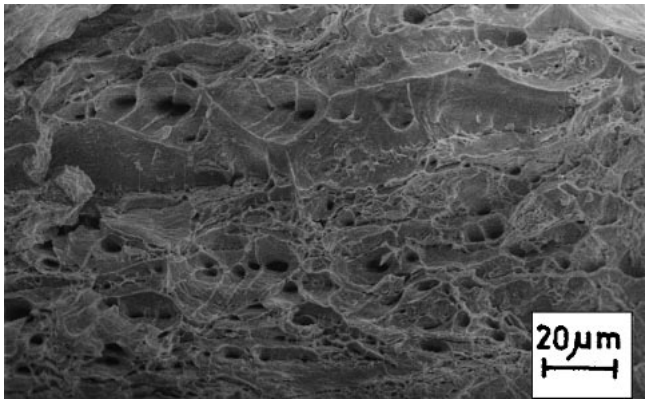

Fig. 11 SEM fractograph of the sample annealed at 860 °C in the lab

fracture mode, as exhibited by cleavage, is shown for the annealing temperature of 980 °C (Fig. 14). These fractographs are in line with the impact values shown in Fig. 10. For comparison of the fracture mode of lab-annealed samples with the conventional batch-annealed one, the fractograph of BAF-processed hot band shown in Fig. 15 depicts a completely ductile fracture, and this fracture mode is closer to the fractograph of the sample lab-annealed at 900 °C (Fig. 12).

3.4 Plant Trial Evaluation

The first plant trial was conducted by annealing a total of 10 groups of coils at 990 °C at line speeds of 6 mpm (3 groups of

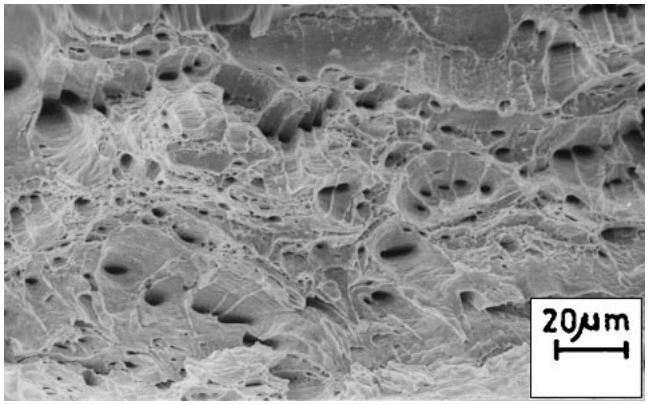

Fig. 12 SEM fractograph of the sample annealed at 900 °C in the lab

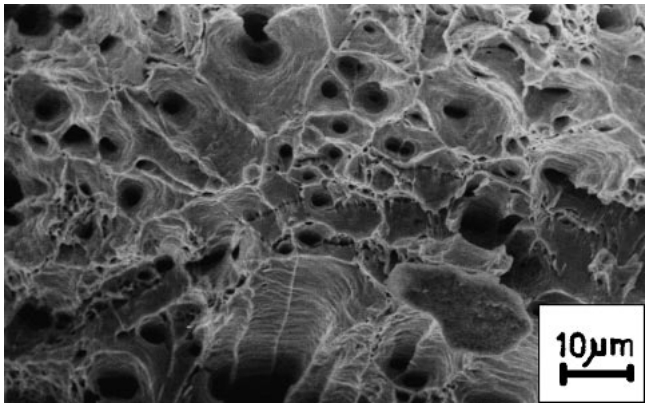

Fig. 13 SEM fractograph of the sample annealed at 940 °C in the lab

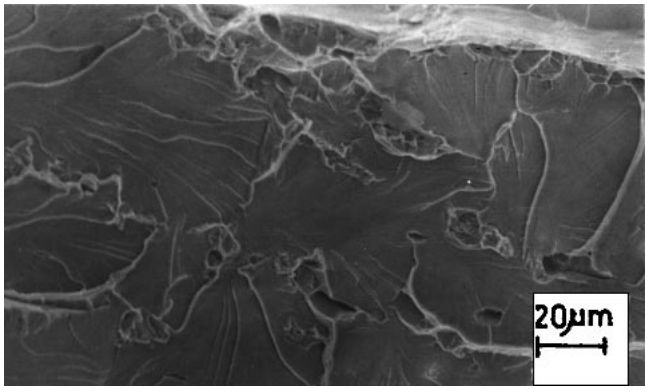

Fig. 14 SEM fractograph of the sample annealed at 980 °C in the lab

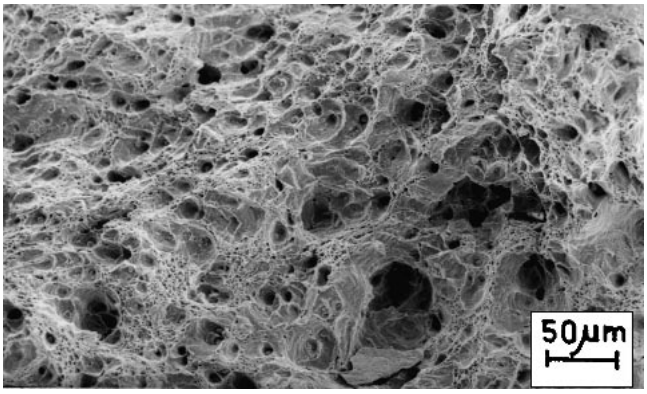

Fig. 15 SEM fractograph of the sample processed through the conventional BAF route

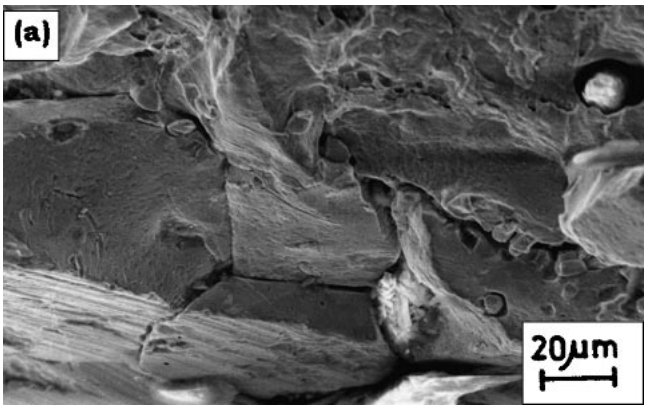

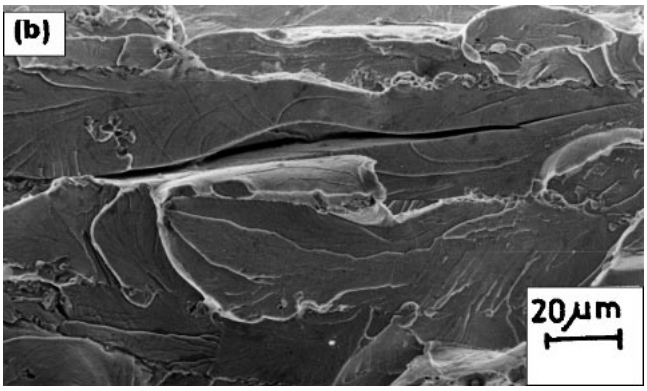

Fig. 16 SEM fractographs of mill-broken sample after annealing at 990 °C and at coil speed of 6 mpm: **(a)** surface, **(b)** center

coils) and 8 mpm (7 groups of coils). As expected, these coils could not be cold-rolled in Z-mill because there was transverse breakage even at the roll bite during the start of the rolling. The fractographs (Fig. 16a and b) of the mill-broken sample indicate the predominance of intergranular fracture and cleavage fracture near the surface and central regions of the annealed HB, respectively. The cleavage fracture is also associated with interband cracks. From Fig. 16 and 5, it can be concluded that the formation of excessive martensite (volume fraction 25%), mostly along ferrite grain boundaries and interband boundaries, and the retention of more carbon in solid solution are the main reasons for the breakage of the annealed coils during Z-mill rolling. The impact value of the continuous-annealed HB was found to be 1.0 kg·m/cm^2, which is similar to the value obtained for lab-annealed at 980 °C (Fig. 10). The brittle fracture mode as shown in Fig. 16 is also similar to Fig. 14 for the lab-annealed sample.

On the other hand, the second plant trial was performed on two groups of coils by annealing at 900 °C and at line speeds

Table 1 Mechanical Properties of Finished Strip (0.5 mm Thickness) Processed Through Hot Band of BAF and CAF Routes

Processing Route	Y.S. (MPa)	U.T.S. (MPa)	Total Elongation (%)	Y.S./ U.T.S Ratio	*r*	*n*	Roping Index
BAF	337.15	468.40	30.0	0.72	0.94	0.18	4.0 to 5.0
CAF	317.53	472.04	28.0	0.67	0.94	0.20	1.0 to 2.0

of 8 and 10 mpm. The pickled coils were then cold-rolled successfully from 4.0 mm to 2.0 mm (reduction ~50%) in the Z-mill. The impact value of this continuously annealed hot band was 13.0 kg · m/cm^2, which is closer to that achieved in the sample lab-annealed at 900 °C (Fig. 10). This clearly shows that the impact value of annealed hot band is an important parameter to assess the further cold rollability of HB. After the first stage of cold rolling, the coils were subjected to an intermediate annealing (temperature 850 °C, line speed 8 mpm). These annealed coils, after pickling, were further cold-rolled to a finish gauge of 0.5 mm thick (reduction ~75%) and then finally annealed at 850 °C at coil speed of 28 mpm before being skin passed (i.e., five passes) as finished products. Table 1 gives the mechanical properties of the finished sheet after processing the annealed HB through CAF and BAF, respectively. The mechanical properties of the finished sheets processed through continuous annealing of HB were found to be comparable or even better to the conventionally processed batch annealing route. However, the roping index, which is a measure of the surface property of the strip, drastically decreased from a level of 4.0 to 5.0 for BAF to 1.0 to 2.0 for CAF. It can be concluded that the annealing temperature and the coil speeds used for the second trial were optimum for continuous hot band annealing.

3.5 Fabrication Trial

About 10 groups of washing-machine top lids were formed successfully from the finished sheet under moderate forming conditions. Figure 17 shows the photograph of one such top lid. It is clear from this figure that the formed components were free from surface defects such as stretcher strains and roping phenomenon.

4. Conclusions

- Impact toughness value provides a guideline for avoiding the breakage of the coils during cold rolling. The crucial value in the current investigation has been found to be 5-6 kg · m/cm^2, below which strip breakage may occur.
- The processing conditions for annealing the hot bands of AISI 430 grade in the continuous annealing furnace have been optimized and are as follows: temperature 900-910 °C and line speed 8-10 mpm. In no case is an annealing temperature above 920 °C recommended.

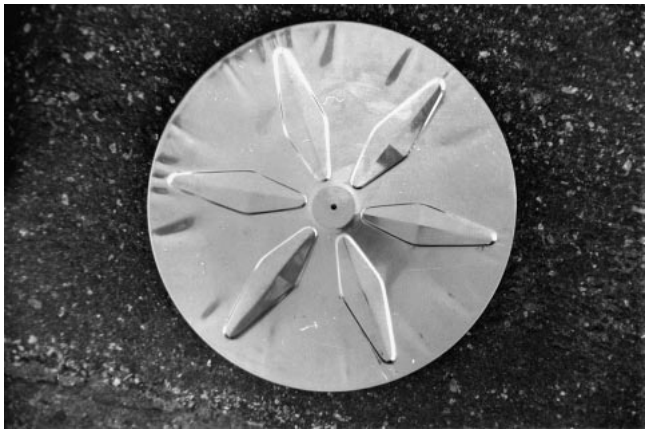

Fig. 17 Photograph of washing-machine top lid

- The two-phase annealing at 900 °C has resulted in the considerable weakening of texture and microstructure of the hot band, in contrast to single-phase annealing.
- The mechanical properties of finished cold-rolled strip produced from the continuous hot band annealing route showed a significant reduction in roping index, as compared to strips produced from conventional batch-annealed hot bands. The mechanical properties for both cases were found to be comparable.

Acknowledgments

The authors would like to express their gratitude to the management of RDCIS, SAIL, Ranchi and Salem Steel Plant, Salem, for their support and inspiration during this work.

References

1. M. Arakawa, S. Takemura, and T. Oaka: Proc. ICSTICS, Suppl. Trans. ISIJ, 1971, *2*, p. 890.
2. T. Sawatani: *Nippon Steel Tech. Rep.*, 1983, *21*, p. 275.
3. T. Sawatani: *Tetsu-to-Hagane*, 1977, *5*, p. 843.
4. T. Sawatani: *Tetsu-to-Hagane*, 1979, *8*, p. 1149.
5. H.C. Chao: *Trans. ASM*, 1967, *60*, p. 37.
6. R.N. Wright: *Metall. Trans. A*, 1972, *3*, p. 83.
7. H. Takechi, H. Kato, T. Sunami, and T. Nakayama: *Trans. Jpn. Inst. Met.*, 1967, *8*, p. 233.
8. R.M. Davison: *Metall. Trans. A*, 1974, *5*, p. 2287.
9. R.M. Davison: *Metall. Trans. A*, 1975, *6*, p. 2243.
10. M. Yamada and Y. Tokunaga, *Trans. ISIJ*, 1985, *25*, p. S460.
11. T. Sawatani, M. Ishü, H. Yoshimura, and J. Harase: U.S. Patent No. 4,515, 644, 1985.
12. P. Viallon and J. Heretier: *Centre de Research Bulletin,* Creusot-Loire, 1977, p. 231.
13. Y. Itoh, K. Okajama, H. Maede, and K. Tashiro: *Trans. ISIJ*, 1982, *22*, p. 223.
14. K. Tashiro, Y. Ikehara, T. Yanai, and S. Matsumura: *Trans. ISIJ*, 1982, *22*, p.255.
15. J.H. Waxweiler: Canada Patent No. 697,689, 1962.
16. P.L. Chalk: U.S. Patent No. 2,055,461, 1969.
17. J. Harase, I. Heno, and T. Nagaie: *Trans. ISIJ*, 1983, *23*, p. S625.
18. C.D. Singh: *Textures Microstruct.*, 1996, *26-27*, p. 445.
19. L.G. Schulz: *J. Appl. Phys.*, 1949, *20*, p. 1030.
20. H.J. Bunge: *Texture Analysis in Materials Science*, Butterworths, London, 1982.
21. C.D. Singh: Ph.D. Thesis, Banaras Hindu University, India, 1989.